The CIDA-QUEST Large-Scale Survey of Orion OB1: Evidence for Rapid Disk Dissipation in a Dispersed Stellar Population

César Briceño,[1]* A. Katherina Vivas,[2] Nuria Calvet,[1,3]
Lee Hartmann,[3] Ricardo Pacheco,[1,4] David Herrera,[1]
Lysett Romero,[1] Perry Berlind,[3] Gerardo Sánchez,[1]
Jeffrey A. Snyder,[2,5] Peter Andrews[5]

We are conducting a large-scale, multiepoch, optical photometric survey [Centro de Investigaciones de Astronomía–Quasar Equatorial Survey Team (CIDA-QUEST)] covering about 120 square degrees to identify the young low-mass stars in the Orion OB1 association. We present results for an area of 34 square degrees. Using photometric variability as our main selection criterion, as well as follow-up spectroscopy, we confirmed 168 previously unidentified pre–main sequence stars that are about 0.6 to 0.9 times the mass of the sun ($M_\odot$), with ages of about 1 million to 3 million years (Ori OB1b) and about 3 million to 10 million years (Ori OB1a). The low-mass stars are spatially coincident with the high-mass (at least 3 $M_\odot$) members of the associations. Indicators of disk accretion such as Hα emission and near-infrared emission from dusty disks fall sharply from Ori OB1b to Ori OB1a, indicating that the time scale for disk dissipation and possibly the onset of planet formation is a few million years.

Exciting discoveries in recent years have deepened our understanding of star and planet formation, including direct images of dusty disks surrounding very young stars (*1, 2*); detection of emission at mid-infrared and submillimeter wavelengths from disks around nearby, more evolved, stars (*3*); and the burgeoning number of extrasolar planets (*4, 5*). However, despite substantial progress, many aspects of star and planet formation remain unknown. Addressing these issues requires observational efforts that go beyond small-scale studies targeting the youngest stars in dark star-forming clouds or in the few very nearby systems (*6*). Somewhat older stars in dispersed stellar populations also must be studied, in comparison with their recently born siblings in dark clouds, to determine the time scales for the coagulation of dust grains into larger bodies such as planets. These older stellar populations are difficult to find because they are widely spread over the sky; their natal dark, dusty molecular clouds have been dispersed and so no longer serve as markers of their positions. Large-scale, spatially unbiased surveys are needed to find these stars.

To address this problem, we started a long-term optical variability survey of large areas in nearby star-forming regions north of declination $-37°$ to find, map, and study large numbers of widely dispersed, low-mass [$\leqslant 2$ solar masses ($M_\odot$)] stars with ages from 1 million to $\sim$20 million years (Ma). In the initial phase of the project, we are conducting a large-scale optical photometric and spectroscopic survey of $\sim$120 square degrees covering the Orion OB1 association. This area (Fig. 1) includes young regions of star formation and older regions devoid of molecular gas. The Orion OB1 subassociations OB1a and OB1b are thought to have ages of $\sim$11 Ma for OB1a and 2 Ma for OB1b, based on the high-mass stars (*7–11*), whereas the compact clusters New General Catalog (NGC) 2024 and the Orion nebula cluster (ONC) are 1 Ma or less.

Although the high-mass stars in Orion OB1 have been studied extensively, relatively little is known about the low-mass stellar population. Existing studies (optical and infrared) of low-mass stars have concentrated mostly on small regions such as the ONC (*12–15*), the surroundings of the star σ Ori (*16*), and selected small fields in OB1a and OB1b (*17*). The Kiso objective prism survey (*18–21*), which covered a very large area, detected some 1200 stars that exhibit the hydrogen Hα emission line at 0.6563 μm, typical of young low-mass stars, but this survey was biased toward the stars with the largest Hα emission fluxes. Studies using the ROSAT All-Sky Survey (RASS) (*22*) have found x-ray–emitting sources over a wide region in Orion, but these samples are strongly contaminated by older foreground field stars unrelated to the young population of Orion (*23, 24*) and do not include the faint $\sim$10-Ma low-mass stars in this region.

Fig. 1. A mosaic of Palomar Observatory Sky Survey optical plates of the Orion OB1 association, with superposed contours of molecular gas (^{12}CO) emission (*47*). Some relevant features are marked, such as the well-known stars in the Orion "belt," δ, ε, and ζ Ori. The bright emission nebulae in the molecular clouds are associated with the ONC and the NGC 2023 and 2024 clusters (located near dense gas concentrations as indicated by the CO peaks), which mark the sites of very recent star formation. The approximate limits of the Orion OB1 subassociations OB1a and OB1b (*9, 10*) are also shown with white dashed lines. The black dashed lines indicate the strip studied here.
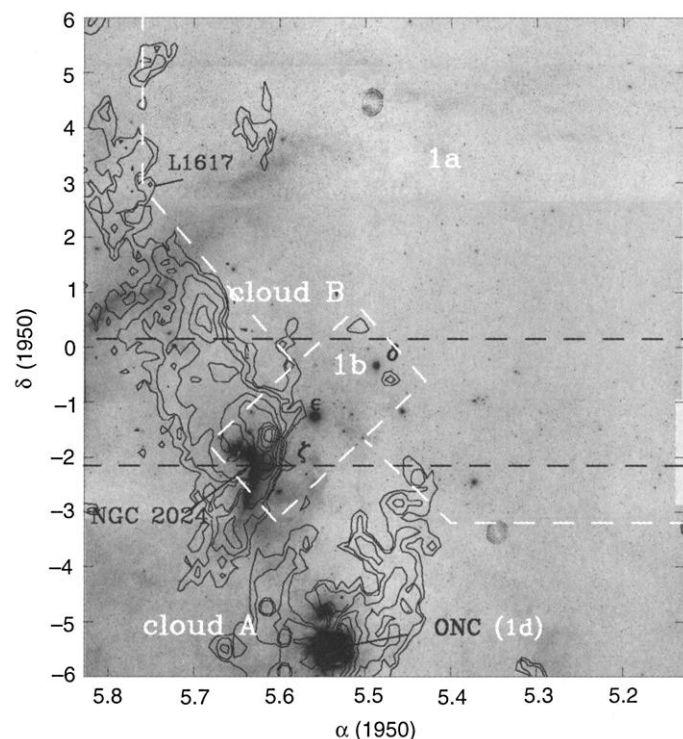
[1]Centro de Investigaciones de Astronomía, Apartado Postal 264, Mérida 5101-A, Venezuela. [2]Department of Astronomy, Yale University, New Haven, CT 06511, USA. [3]Harvard-Smithsonian Center for Astrophysics, Cambridge, MA 02138, USA. [4]Physics Department, Universidad de los Andes, Mérida 5101, Venezuela. [5]Department of Physics, Yale University, New Haven, CT 06520, USA.

*To whom correspondence should be addressed. E-mail: briceno@cida.ve

Our survey for low-mass young stars in Orion is unique in its repeated observation of large areas of the sky. The survey is being carried out with the Quasar Equatorial Survey Team (QUEST) 8000 by 8000 pixels charge-coupled device (CCD) mosaic camera (25), which is installed on the 1-m (clear aperture) Schmidt telescope at Llano del Hato Observatory, in the Venezuelan Andes (8°47'N, 70°52'W, 3610-m elevation). The 16 2048 by 2048 CCD chips are set in a 4 by 4 array, yielding a scale of 1.02" per pixel and a field of view of 2.3° by 2.3° (26). Four filters can be accommodated, each covering the north-south columns of four CCD chips. The camera is optimized for drift-scan observing in the range $-6° \leq \delta \leq 6°$ (δ, declination); the telescope is fixed and the CCDs are read out east to west at the sidereal rate as stars drift across the device, crossing each of the four filters in succession. This procedure generates a continuous strip (or "scan") of the sky at a rate of 34.5 square degrees per hour per filter; the faintest stars detected have a limiting magnitude in the visual band $V_{lim} = 19.7$ with a signal-to-noise ratio of 10. Repeated multiband observations allow us to single out objects that have varied their brightness over time scales of days up to a few weeks. Because all pre–main sequence stars are variable (27), variability can be used as an efficient technique to select pre–main sequence stars from among the vast numbers of foreground and background stars.

Here, we present preliminary results for the first 2.3° wide by 9.7° long strip, centered at declination of about −1°, covering a portion of Ori OB1a, most of Ori OB1b, and a region over cloud B. Our first observations consisted of 16 BVR_cI_c (28) scans over the strip indicated in Fig. 1, obtained during December 1998 to early February 1999. Each of

the ~100,000 stars in our survey area has, on average, 12 to 15 data points during this period, with the missing ones being rejected because of bad columns, cosmic rays, etc. We calibrated a "master" scan using standard fields (29) and then normalized the photometry in all other scans to this reference scan. We developed tools for identifying variable stars using differential photometry. The typical photometric errors are 0.02 magnitude for visual magnitude $V \sim 16$ and ~ 0.08 magnitude at $V \sim 19$. With a χ^2 test and assuming a Gaussian distribution for the errors, we consider variable only those objects for which the probability that the observed distribution is a result of the random errors is <0.01%. Thus, the minimum amplitude we can detect at a 99.99% confidence level is $\Delta V \sim 0.07$ magnitude at $V \sim 16$ and $\Delta V \sim 0.4$ magnitude at $V \sim 19$ (we are presently observing all objects, variable and nonvariable, in selected areas to quantify the completeness of our sample).

Potentially young variable stars, which are above the zero-age main sequence (ZAMS) in the color-magnitude diagram [Fig. 2B (30)], are well separated from those below the ZAMS (mostly foreground/background main sequence stars). In contrast, this separation is much less clear in a plot including all stars (Fig. 2A), emphasizing the value of variability over photometry alone to pick up pre–main sequence candidates. Out of ~4000 potential candidates above the main sequence, ≲10% are variables, reducing the number of stars to be studied with follow-up spectroscopy.

There are only five previously known, low-mass pre–main sequence stars in this region (31) [also known as T Tauri stars (TTS)], and all were detected as variables. In addition, 151 Kiso Hα stars (18–21) lie with-

in our survey area. Of the 58 Kiso stars located above the ZAMS, ~70% are detected as variables; essentially none of the ones below the ZAMS are variables [they could be a mixture of field dMe stars (32) and some false detections (24)]. Our results show that the Kiso survey is strongly contaminated by main sequence stars. Only nine of the sources identified by the RASS study of Orion (22) as new weak T Tauri stars (WTTS) fall within our study area; all are too bright ($V \lesssim 13.6$) for our survey, being saturated in our CCD data.

Confirmation of the pre–main sequence nature of candidate stars is accomplished by follow-up spectroscopy, using emission lines such as Hα and the absorption line Li I at 0.6707 μm for stars of spectral types later than about K4 as indicators of youth (23, 24). Here, we discuss the brighter ($V \lesssim 16$) candidates, for which spectra were obtained with the fast spectrograph for the Tillinghast telescope (FAST) (33) on the 1.5-m telescope of the Smithsonian Astrophysical Observatory at Mount Hopkins, with a spectral resolution of 0.00065 μm covering the spectral range of 0.4 to 0.7 μm. Of 320 candidates, 168 are confirmed spectroscopically as low-mass pre–main sequence stars. The remaining objects are a mixture of mostly background stars of late G to K spectral type (some giants included) and field dMe stars.

Masses and ages of the stars can be estimated from comparison of the optical data with theoretical evolutionary tracks if the distances are known. Distances are needed to place lines of constant age (isochrones) and constant mass (tracks) in a color-magnitude diagram (Fig. 3). We adopted the average distances derived from the Hipparcos satellite (34), 330 pc (35) to OB1a and 440 pc to OB1b, with formal uncertainties of 5%, although these are lower limits and an intrinsic spread of the order of 100 pc may exist. We assigned each star to associations OB1a or OB1b or to Cloud B, according to its projected position in the sky and comparison with the location of the O and B type stars in each association (Fig. 1).

Color-magnitude diagrams for stars in Ori OB1a and OB1b are shown in Fig. 3 (36), along with evolutionary tracks for masses 0.3 to 1 $M_\odot$ and isochrones for 1 to 100 Ma (37) adjusted to the distances given above. We also indicate the correction in the diagram needed to account for 1 magnitude of extinction (38). Magnitudes and colors for each star are median values determined from the multiple observations of each object. The median amplitude of the variability in the visual band is 0.3 magnitudes, although some of the more active stars show a larger spread of up to 1.7 magnitudes. Because the variations in each star are uncorrelated with the others, they
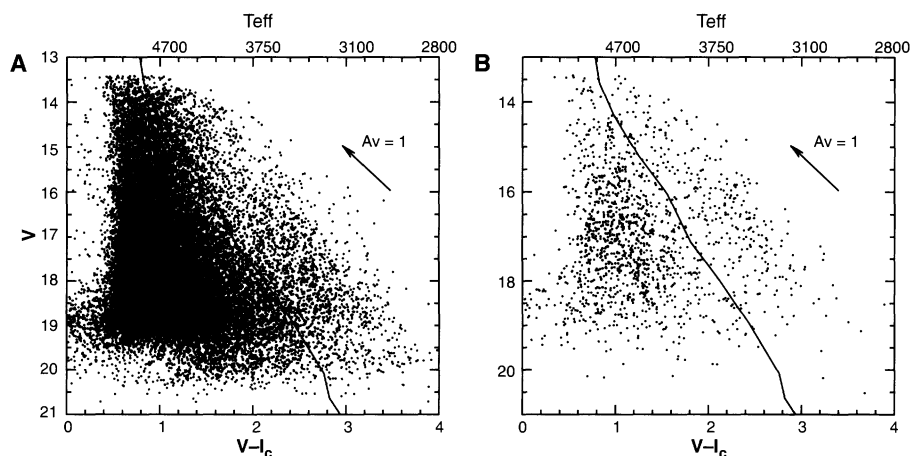

Fig. 2. V versus ($V − I_c$) diagram for different samples in an ~10 square degree area within Ori OB1b for (**A**) all stars and (**B**) variable stars only. The data shown correspond to one epoch (reference scan). The solid line indicates the ZAMS at the assumed distance of 460 pc. The arrow indicates the shift of a star's position in the diagram for a 1-magnitude correction in visible extinction (A_V). The scale at the top of (A) and (B) indicates the equivalent surface temperature of the star in degrees kelvin (T_{eff}).

do not affect the location of the sample as a whole in the color-magnitude diagram. There is a large spread in the apparent ages for stars of a given association, which may be partly due to a spread in distance. In addition, contamination of one group by members of the other may occur, because the boundaries of each group may overlap. However, even given these uncertainties, it is apparent that stars in 1a are older than stars in OB1b. Stars in OB1b seem to fall between the isochrones corresponding to 1 to 3 Ma, whereas stars in OB1a seem to fall between 3 and 30 Ma, in agreement with photometric age estimates for the high-mass stars of the associations. Thus, our results confirm the general difference in population ages found from studies of the massive stars. The new TTS have spectral types K2 to M2, corresponding to masses of ~0.9 to 0.6 $M_\odot$.

According to our present understanding, protoplanetary disks accrete onto their central stars over time scales of millions of years. Accretion onto the star results in strong Hα emission (39), whereas dust in the innermost disk emits at near-infrared wavelengths (40). The epoch of planet formation is thought to be similar to the time that accretion stops, either because the planet(s) have removed accreting, viscously evolving disk material or because the dispersal of disk material halts both accretion and planet formation (41). Thus, the disappearance of near-infrared dust emission and accretion-related Hα emission may be taken as signposts for the onset of planet formation. The probable time scale for this process, based on both meteoritic and limited astronomical observational evidence, is thought to be of the order of 10 million years (42), thus the OB1a and OB1b sub-groups can provide further constraints on this mechanism.

The distribution of the equivalent widths of the Hα emission for Ori OB1a and OB1b is shown in Fig. 4. The value of 10 Å for the Hα equivalent width has traditionally been taken as the dividing line between the classical T Tauri stars (CTTS), still accreting material from their surrounding disks, and the WTTS, where accretion has stopped and the remnant emission is due to stellar magnetic activity. Essentially all the stars are nonaccreting WTTS in Ori OB1a, whereas the accreting CTTS are found in OB1b. Formally, the fraction of CTTS/WTTS is 0.05 in OB1a and 0.20 in OB1b, although the latter must be considered as a lower limit because of the possibility that stars from OB1a are contaminating the result.

We have obtained near-infrared J, H, and K (43) magnitudes of the new pre–main sequence stars from the second release of the Two Micron All Sky Survey (2MASS). The $J - H$ versus $H - K$ diagram for our

sources, along with expected colors for dwarfs and giants, is shown in Fig. 5. All stars in Ori OB1a are within the region expected for purely stellar emission, allow-

ing for small amounts of extinction. In contrast, a substantial number of stars in OB1b have much larger $H - K$ colors, indicating excess disk emission; many lie
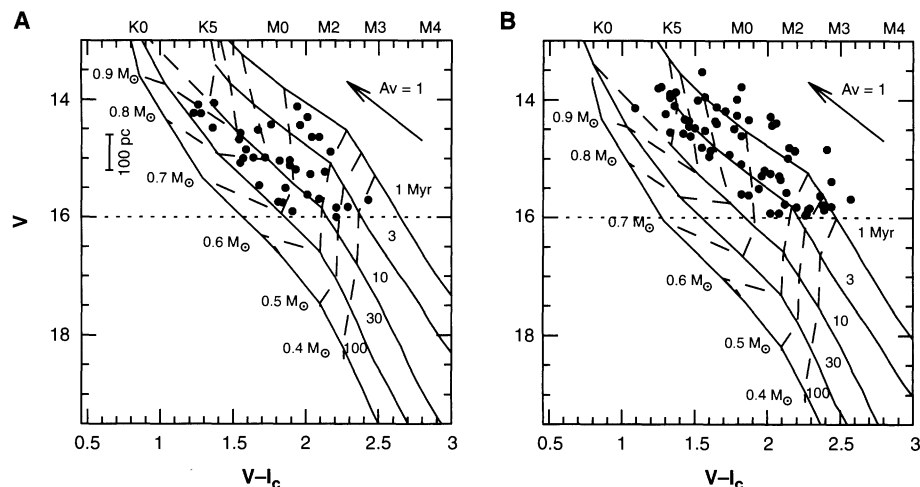

Fig. 3. V versus $(V - I_c)$ diagram for (**A**) Ori OB1a and (**B**) Ori OB1b. The assumed distances are 330 pc (for OB1a) and 460 pc (for OB1b). Isochrones (solid lines) for ages 1 to 100 Ma and evolutionary tracks (dashed lines) for masses 0.4 to 0.9 $M_\odot$ (30) are indicated. The shifts due to 1 magnitude of de-reddening (arrow) and to a distance change of 100 pc (left vertical bar) are also indicated. The dotted line shows the limiting magnitude for the FAST spectroscopy reported here. At the top of (A) and (B), the equivalent spectral types are indicated.

Fig. 4. Fraction of stars with given Hα equivalent width (EW) in (**A**) Ori OB1a and (**B**) Ori OB1b. Units of the equivalent width are in angstroms (1 Å = 10^{-10} m). Large values of Hα equivalent width only appear in OB1b. The vertical dotted line indicates the canonical EW(Hα) = 10 Å separation between CTTS and WTTS.
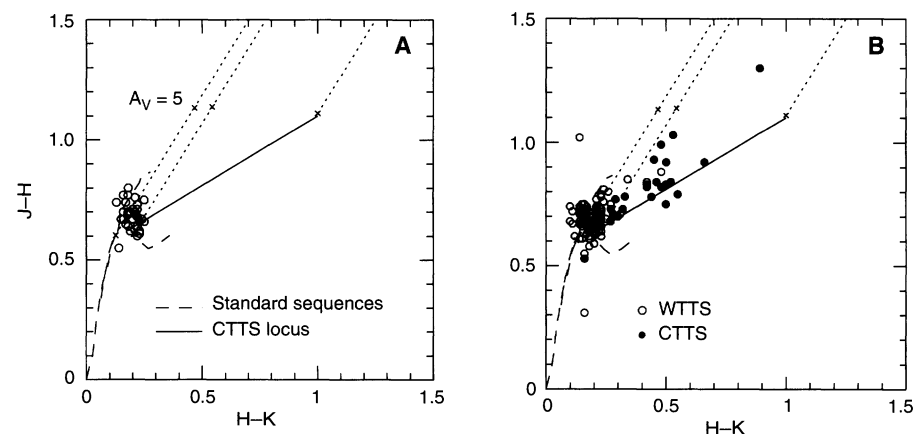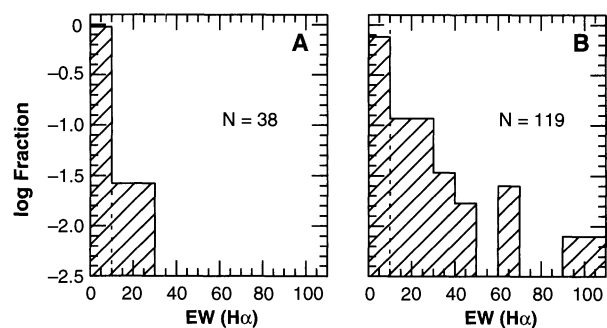

Fig. 5. $J - K$ versus $H - K$ diagram for (**A**) Ori OB1a and (**B**) Ori OB1b. JHK data are from 2MASS. The dwarf and giant standard sequences are indicated (dashed lines), as well as the location of the accreting stars, the locus of the CTTS (solid lines). The shift in colors due to reddening is indicated by dotted lines, with crosses at $A_V = 5$. Reddening shifts are indicated for a K7 star, an M2 star (approximately the latest spectral type in our sample), and the red end of the locus. All stars in OB1a are inside the reddening line corresponding to M2. In contrast, the locus of the CTTS is substantially populated in OB1b. All but one (probably a binary) of the OB1b stars on the locus are CTTS (solid circles), as determined by their Hα equivalent width.
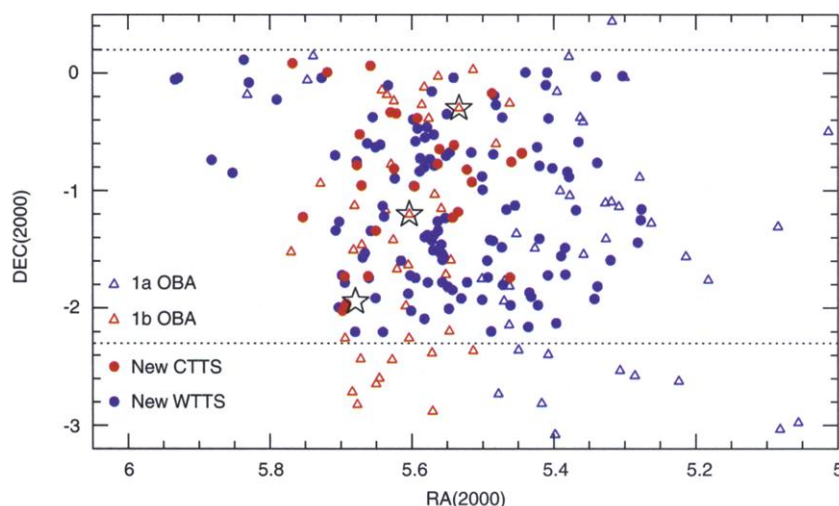
Fig. 6. Spatial distribution of previously unidentified TTS (solid symbols) compared to Hipparcos-selected stars of O, B, and A spectral types in OB1a (blue open triangles) and in OB1b (red open triangles). The position of the belt stars (large star symbols) and the limits of the scan (dotted lines) are indicated as reference. There is a sharp cutoff in the low-mass star distribution at low right ascension (RA), consistent with the distribution of high-mass stars. Also, there is a concentration of the previously unidentified CTTS (solid red dots) toward OB1b.

near the "CTTS locus" of young stars with accretion disks (40). All but one of the stars with infrared excesses have the strong Hα emission associated with accretion. The disappearance of Hα and near-infrared emission in OB1a stars indicates that protoplanetary disk accretion stops for almost all solar-type stars on a time scale of a few million years. This result is consistent with the lack of disk accretion among most of the stars in the 10-Ma stars of the TW Hya association (44) but with greater statistical significance, due to our much larger sample.

Finally, we consider the implications of our preliminary results for the star formation history of the region. In Fig. 6, we compare the location of the previously unidentified stars in the sky with that of the proper motion/parallax–selected OB members of the associations (34). The east-west boundaries of the low-mass members of the association are remarkably well defined and agree well with the spatial distribution of the higher mass stars. This cannot be a selection effect, because our scans extend well beyond the stellar distribution on either side with similar sensitivity. Our results show no evidence for a widely spread population of stars dispersed from the present-day molecular clouds in the region; instead, we find a well-defined older association that is the remnant of a no longer existing molecular cloud complex, consistent with our interpretation of surveys of young stars detected with the ROSAT satellite (22). The absence of molecular gas in Ori OB1a supports suggestions that large molecular cloud complexes can form stars and disperse quickly, in only a few million years (45, 46).

References and Notes

1. C. R. O'Dell, Z. Wen, X. Hu, *Astrophys. J.* **410**, 696 (1993).
2. E. Pantin, C. Waelkens, P. O. Lagage, *Astron. Astrophys.* **361**, L9 (2000); G. Fazio, *Astrophys. J. Lett.* **503**, 79 (1998).
3. D. J. Wilner, P. T. P. Ho, J. H. Kastner, L. F. Rodríguez, *Astrophys. J. Lett.* **534**, 101 (2000).
4. R. W. Noyes et al., *Astrophys. J.* **483**, 111 (1997).
5. D. Queloz et al., *Astron. Astrophys.* **354**, 99 (2000).
6. J. H. Kastner, B. Zuckerman, D. A. Weintraub, T. Forveille, *Science* **277**, 67 (1997).
7. A. Blaauw, *Annu. Rev. Astron. Astrophys.* **2**, 213 (1964).
8. A. Blaauw, in *The Physics of Star Formation and Early Stellar Evolution*, C. Lada, N. D. Kylafis, Eds. (Kluwer, Dordrecht, Netherlands, 1991), pp. 125–152.
9. W. H. Warren, J. E. Hesser, *Astrophys. J. Suppl. Ser.* **34**, 115 (1977).
10. ———, *Astrophys. J. Suppl. Ser.* **36**, 497 (1978).
11. A. G. A. Brown, E. J. de Geus, P. T. de Zeeuw, *Astron. Astrophys.* **289**, 101 (1994).
12. L. Hillenbrand, *Astron. J.* **113**, 173 (1997).
13. K. G. Stassun, R. D. Mathieu, T. Mazeh, F. J. Vrba, *Astron. J.* **117**, 2941 (1999).
14. M. J. McCaughrean, J. R. Stauffer, *Astron. J.* **108**, 1382 (1994).
15. B. Ali, D. L. Depoy, *Astron. J.* **109**, 709 (1995).
16. F. M. Walter, S. J. Wolk, W. Sherry, in *The Tenth Cambridge Workshop on Cool Stars, Stellar Systems and the Sun*, R. A. Donahue, J. A. Bookbinder, Eds., vol. 154 of *ASP Conference Series* (Astronomical Society of the Pacific, San Francisco, 1998), pp. 1793–1799.
17. W. Sherry, F. M. Walter, S. J. Wolk, *Bull. Am. Astron. Soc.* **194**, 68.14 (1999).
18. S. D. Wiramihardja et al., *Publ. Astron. Soc. Jpn.* **43**, 27 (1991).
19. S. D. Wiramihardja, T. Kogure, S. Yoshida, K. Ogura, M. Nakano, *Publ. Astron. Soc. Jpn.* **45**, 643 (1993).
20. T. Kogure et al., *Publ. Astron. Soc. Jpn.* **41**, 1195 (1989).
21. M. Nakano, S. D. Wiramihardja, T. Kogure, *Publ. Astron. Soc. Jpn.* **47**, 889 (1995).
22. J. M. Alcalá et al., *Astron. Astrophys. Suppl. Ser.* **199**, 7 (1996).
23. C. Briceño et al., *Astron. J.* **113**, 740 (1997).
24. C. Briceño, N. Calvet, S. Kenyon, L. Hartmann, *Astron. J.* **118**, 1354 (1999).
25. The QUEST collaboration involves Yale University, Indiana University, Centro de Investigaciones de As-
tronomía (CIDA), and Universidad de Los Andes (Venezuela).
26. J. A. Snyder et al., *Proc. SPIE* **3355**, 635 (1998).
27. G. H. Herbig, in *Problems of Physics and Evolution of the Universe*, L.V. Mirzoyan, Ed. (Armenian Academy of Sciences, Yerevan, Armenia, 1978), pp. 171–180.
28. The blue (*B*), visual (*V*), red (*R*c), and *I*c bandpasses in the Johnson-Cousins photometric system are defined by their central wavelengths and half widths (in μm), respectively, as follows: *B*, 0.44 and 0.1; *V*, 0.55 and 0.09; *R*c, 0.64 and 0.18; and *I*c, 0.79 and 0.14.
29. A. U. Landolt, *Astron. J.* **104**, 340 (1992).
30. Normally, a Hertzsprung-Russell (H-R) diagram plots the spectral type, or surface temperature, of a star against the star's intrinsic luminosity; theoretical models describe the evolution of stars of various masses on this diagram. But, there is a correspondence between the star's temperature and its color, given by Wien's Law, $\lambda_{max} = 0.28978$ cm·K (λ_{max} = wavelength of maximum flux). A star's color can be determined by measuring its brightness through two different filters. We can therefore plot the color of a star against its brightness (measured in magnitudes) as a way of building an "observational" H-R diagram, known as a color-magnitude diagram.
31. G. H. Herbig, K. R. Bell, *Lick Obs. Bull.* **1111**, 1 (1988).
32. Dwarf M-type stars, with emission in the hydrogen Hα line, or dMe stars have surface temperatures lower than ~3800 K and typical equivalent widths in Hα ≤ 10 Å. They belong to the general disk population of our Galaxy, with ages of ~0.5 × 10⁹ to 2 × 10⁹ years.
33. The FAST spectrograph is described in work by D. Fabricant, P. Cheimets, N. Caldwell, and J. Geary [*Publ. Astron. Soc. Pac.* **110**, 79 (1998)].
34. A. G. A. Brown, F. M. Walter, A. Blaauw, in *The Orion Complex Revisited*, M. J. McCaughrean, A. Burkert, Eds., *ASP Conference Series*, in press.
35. The equivalent of 1 pc is 3.086 × 10¹⁶ m.
36. Here, we discuss results for these two subassociations, deferring the discussion for stars on Cloud B.
37. I. Baraffe, G. Chabrier, F. Allard, P. H. Hauschildt, *Astron. Astrophys.* **337**, 403 (1998).
38. Because the extinction moves stars roughly parallel to the isochrones, it will not affect our age estimates significantly, although masses could be higher.
39. J. Muzerolle, N. Calvet, L. Hartmann, *Astrophys. J.* **492**, 74 (1998).
40. M. Meyer, N. Calvet, L. Hillenbrand, *Astron. J.* **114**, 288 (1997).
41. D. N. C. Lin, J. C. B. Papaloizou, in *Protostars and Planets III*, E. H. Levy, J. I. Lunine, Eds. (Univ. of Arizona Press, Tucson, 1993), pp. 749–835.
42. F. A. Podosek, P. Cassen, *Meteoritics* **29**, 6 (1994).
43. The *J*, *H*, and *K*-short bandpasses of the 2MASS photometric system are defined by their central wavelengths and half widths (in μm), respectively, as follows: *J*, 1.25 and 0.26; *H*, 1.65 and 0.29; and *K*s, 2.17 and 0.32.
44. J. Muzerolle, N. Calvet, C. Briceño, L. Hartmann, L. Hillenbrand, *Astrophys. J. Lett.* **535**, L47 (2000).
45. J. Ballesteros-Paredes, L. Hartmann, E. Vázquez-Semadeni, *Astrophys. J.* **527**, 285 (1999).
46. B. G. Elmegreen, *Astrophys. J.* **530**, 277 (2000).
47. R. Maddalena, M. Morris, J. Moscowitz, P. Thaddeus, *Astrophys. J.* **303**, 375 (1987).
48. We acknowledge support from NSF grant AST-9987367. Research reported herein is based on observations made with the 1-m Schmidt Telescope at Observatorio Astronómico Nacional de Llano del Hato, Mérida, Venezuela, operated by CIDA and funded by the Ministerio de Ciencia y Tecnología and the Consejo Nacional de Investigaciones Científicas y Tecnológicas of Venezuela. This report makes use of data products from 2MASS, which is a joint project of the University of Massachusetts and the Infrared Processing and Analysis Center at the California Institute of Technology, funded by NASA and NSF.